JOURNAL OF GUIDANCE, CONTROL, AND DYNAMICS
Vol. 22, No. 4, July–August 1999

Implementation of Optimal Guidance Laws Using Predicted Missile Velocity Profiles

Hangju Cho* and Chang Kyung Ryoo†
Agency for Defense Development, Taejon 305-600, Republic of Korea
and
Min-Jea Tahk‡
Korea Advanced Institute of Science and Technology, Taejon 305-701, Republic of Korea

A class of weighted control-effort minimizing guidance laws are derived for missiles of varying velocity. As a practical weighting function, we consider a function of air density and missile velocity parameterized by positive real numbers. The resulting optimal guidance problem can be interpreted as the drag minimization problem for subsonic or supersonic missiles, depending on what parameters are used. This approach is extended easily to solve the drag minimization of a typical antiaircraft missile system with an arbitrary velocity profile and arbitrary drag characteristics, as demonstrated by a simulation study. We also present analytical results on how the guidance gain of the optimal law varies according to the values of the parameters. Because the optimal guidance laws make use of the future missile velocity profile, one critical issue is how to implement the laws. To avoid the difficulty that an inaccurately predicted missile velocity profile causes the guidance command to blow up in the last part of the engagement, we suggest two simple on-line velocity-profile updating schemes, which considerably alleviate the problem.

I. Introduction

THE well-known proportional navigation guidance (PNG) law is optimal for constant-velocity missiles in the sense that it minimizes the control efforts, and it possesses the desirable property that if there is no guidance system lag, the guidance command decreases to zero as the missile approaches the target. When the missile has a nonconstant velocity profile, however, PNG is no longer optimal in any sense and its guidance command often becomes excessively large in the final stage of the engagement, even for the case of no lag in the guidance system. Because typical surface-to-air missiles have large velocity changes in their boosting–coasting flight profiles, there has been a need for studies on proper guidance laws that would explicitly take the missile velocity variation into account.

Recently, Baba et al.[1] proposed a guidance law, where a collision trajectory is computed using the future missile velocity profile and the guidance command is generated to nullify the portion of line-of-sight rate incurred by the deviation of the missile velocity vector from the computed collision trajectory. Cho et al.[2] investigated a control-effort minimizing guidance law for varying-velocity missiles and studied some qualitative properties of the key variables in their guidance law, such as guidance gain and a time-to-go–like function t_g. We extend our previous results[2] and derive in the same optimal guidance framework a class of weighted control-effort minimizing guidance laws that comprise drag minimization laws for subsonic and supersonic missiles and a law that minimizes the control efforts penalized by the inverse of dynamic pressure.

The main thrust of this extension has been an obvious fact that, in many surface-to-air applications, a major limitation of the performance comes from missile velocity that is too low in the final stage of engagement; thus, a drag-minimizing missile trajectory can considerably enhance the overall missile performance. Another practical concern is that because the missile maneuver capability is inversely proportional to the dynamic pressure, it is undesirable to request a high missile maneuver when the dynamic pressure is low; this case calls for a guidance law that discourages guidance activities when the dynamic pressure is low. The optimal guidance laws of this paper differ only in their guidance gains and result in guidance command histories that are sufficiently different from each other to call for a practical designer's attention. We present the results of a comparative study on these guidance laws.

A unique feature of the guidance laws in this paper and of the law of Baba et al.[1] is the use of the future missile velocity profile. Because the future missile velocity profile cannot be determined exactly before the end of engagement, use of some type of predicted velocity profile is required in actual implementation. We therefore study the effect of the use of inaccurately predicted missile velocity profiles and present two simple velocity-profile updating schemes that can effectively remedy the problem. Miss-distance analysis also has been performed for the case of heading error and guidance system lag to assess the performance of the proposed guidance algorithms.

This paper is organized as follows: In Sec. II, the significance of the weighted control-effort minimizing guidance problem is discussed at length, which is followed by the derivation of the guidance laws. In Sec. III, the properties of the guidance gains are investigated to provide some insights into the relation between various weighting functions and the resulting guidance laws. Then, implementation issues concerned mostly with the use of inaccurate velocity profiles are discussed in Sec. IV. The simulation study provided in Sec. V compares the proposed guidance laws with other existing guidance laws in the presence of velocity profile errors. Numerical results also are given for a drag minimization problem of a surface-to-air missile system that starts the homing phase at a subsonic speed but intercepts the target at a supersonic speed. Finally, in Sec. VI are the concluding remarks.

II. Optimal Guidance Laws

Consider the homing guidance geometry shown in Fig. 1. Here, σ_L denotes the flight-path angle for the perfect collision path that is determined at the beginning of engagement and remains fixed throughout the engagement. Other variables in Fig. 1 are self-explanatory. The equations of motion in this homing problem are given by

$$\dot{z}(t) = V_t(t)\sin\sigma_t(t) - V_m(t)\sin\sigma_m(t), \qquad V_m(t)\dot{\sigma}_m(t) = u(t) \tag{1}$$

Received 19 March 1998; revision received 31 December 1998; accepted for publication 3 March 1999.

*Principal Researcher, 3-1-3, P.O. Box 35-3, Yusong.
†Senior Researcher, 3-1-3.
‡Department of Aerospace Engineering, 373-1 Kusong Yusong; mjtahk@fdcl.kaist.ac.kr. Member AIAA.

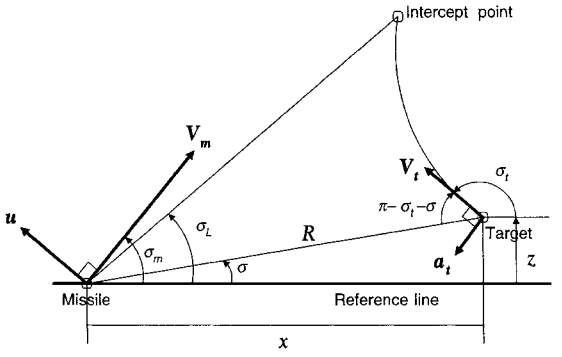

Fig. 1 Homing guidance geometry.

Let us denote the deviation of the missile flight-path angle from σ_L by $\Delta\sigma_m$; i.e., $\Delta\sigma_m \equiv \sigma_m - \sigma_L$. Assuming small $\Delta\sigma_m$, we linearize Eq. (1) about $z=0$ and $\sigma_m = \sigma_L$ and use a new variable V_z defined as

$$V_z \equiv V_t \sin\sigma_t - V_m \sin\sigma_L - V_m \cos\sigma_L \Delta\sigma_m$$

to obtain

$$\begin{aligned} \dot{z}(t) &= V_z(t) \\ \dot{V}_z(t) &= c(t)V_z(t) - c(t)V_{tz}(t) + a_{tz}(t) - u_z(t) \end{aligned} \tag{2}$$

where

$$u_z \equiv u\cos\sigma_L, \qquad c \equiv \frac{\dot{V}_m}{V_m}, \qquad V_{tz} \equiv V_t \sin\sigma_t, \qquad a_{tz} \equiv \frac{\mathrm{d}}{\mathrm{d}t}V_{tz}$$

In our previous study,[2] we considered an optimal guidance problem in which the overall control effort

$$\int_0^{t_f} u_z^2 \,\mathrm{d}t$$

where t_f is a fixed terminal time, is minimized subject to Eq. (2) and the terminal constraint $z(t_f)=0$. We extend the result of Ref. 2 to consider more general cost functions in the framework given earlier. Specifically, we consider a weighted control effort as a cost function that can account for either the overall control-dependent drag force acting on the missile throughout the engagement or the control efforts penalized by the inverse of dynamic pressure.

It is well known that the total drag D on a subsonic finite wing is the sum of the profile drag and the induced drag, and the latter is dependent upon the lift L or, equivalently, the control u_z here. Indeed, if we denote the induced-drag coefficient and the lift coefficient by C_{D_i} and C_L, respectively, then $C_{D_i} = k_i C_L^2$, where the coefficient k_i is almost constant for subsonic flight. When the mass of the missile is considered to be constant, we therefore have

$$\text{Induced drag} \propto \frac{\rho}{2} C_{D_i} V_m^2 \propto \frac{\rho}{2} k_i C_L^2 V_m^2 \propto \frac{k_i L^2}{\rho V_m^2} \propto \frac{k_i u_z^2}{\rho V_m^2}$$

where ρ is the air density. Therefore, minimizing the overall drag while exerting the lift necessary for the interception of the target amounts to minimizing the weighted control effort

$$\int_0^{t_f} \rho^{-1} V_m^{-2} u_z^2 \,\mathrm{d}t$$

subject to the terminal constraint $z(t_f)=0$.

In supersonic flight, a major drag component is the wave drag, and it is known that the wave-drag coefficient C_{D_w} is

$$C_{D_w} = \frac{\sqrt{M^2-1}}{4} C_L^2 + \frac{k_w}{\sqrt{M^2-1}}$$

where M is the Mach number and k_w is a function of the airfoil camber and thickness. In the altitude range where aerodynamic control is applicable, the variation in the speed of sound is less than 13%.[3] Hence, for high supersonic flight, it is reasonable to approximate $\sqrt{(M^2-1)}$ as V_m divided by the speed of sound at some altitude. Reasoning in the same manner as before, we can argue that the drag minimization problem for high supersonic missiles is to minimize

$$\int_0^{t_f} \rho^{-1} V_m^{-1} u_z^2 \,\mathrm{d}t$$

Note that the maneuver capability of a missile is proportional to the dynamic pressure $\rho V_m^2/2$. Hence, we may consider a weight function inversely proportional to the dynamic pressure; the cost function is chosen as

$$\int_0^{t_f} \left(\rho V_m^2\right)^{-\gamma} u_z^2 \,\mathrm{d}t$$

where $\gamma > 0$. This formulation will produce a guidance law that causes the missile to maneuver less when it cannot generate large enough normal forces; such a guidance law will be particularly useful in applications in which the available normal force is marginal when compared to the requirement. In fact, the drag minimization in the subsonic regime is equivalent to the minimization of control effort weighted by the inverse of dynamic pressure ($\gamma = 1$).

The preceding considerations on drag and dynamic pressure lead to a family of cost functions expressed as

$$J = \frac{1}{2}\int_0^{t_f} w(t) u_z^2(t) \,\mathrm{d}t \tag{3}$$

where $w(t) = \rho^{-\alpha}(t) V_m^{-\beta}(t)$. The guidance law studied in Ref. 2 corresponds to the case of $\alpha = \beta = 0$. The minimization of induced drag for a subsonic flight corresponds to $\alpha = 1$ and $\beta = 2$ whereas the drag minimization for a supersonic flight is the case of $\alpha = 1$ and $\beta = 1$. Furthermore, the above formulation can be generalized for the case that the velocity profile includes both subsonic and supersonic speeds. Suppose that the drag coefficient is expressed as

$$C_D = C_{D_o}(M) + k_i(M) C_L^2 \tag{4}$$

where C_{D_o} and $k_i(M)$ are dependent on the Mach number M. As discussed earlier, the induced drag is proportional to $k_i(M)u_z^2/\rho V_m^2$. Therefore, the drag minimization problem for this case is solved easily by choosing the weight function as $w(t) = k_i(M)/\rho V_m^2$. Note that the general drag minimization problem takes the form of the minimization of the control efforts penalized by the inverse of the dynamic pressure ($\gamma = 1$), but the induced-drag coefficient $k_i(M)$ also is involved.

Strictly speaking, ρ and V_m are dependent on the state z and control u_z of our homing system. However, the introduction of such dependency into optimal guidance formulation will lead to the situation in which no closed-form solution is available. However, this difficulty can be avoided by using the predicted profiles of ρ and V_m for guidance command generation. For example, the missile velocity profile can be predicted in advance by using an appropriate drag model. For this purpose, the induced drag may be ignored or calculated from the average control effort required to intercept the target. The density profile is not important when the missile's altitude does not vary significantly. If this is not the case, the density profile can be approximated by assuming that the missile travels along a straight line up to the predicted intercept point. Hence, we now assume that $\rho(t)$ and $V_m(t)$ are given. Implementation issues concerned with inaccurately predicted velocity profiles are discussed in Sec. IV.

Now let us solve the minimization problem of Eq. (3) subject to the dynamic constraint (2) and the terminal constraint $z(t_f)=0$. Here, the weighting function $w(t)$ is assumed to be a strictly positive function of time. The solution of the optimal control problem posed in Eq. (3) can be obtained in a straightforward manner (e.g., see Ref. 4) and given as

$$u_z = w^{-1} B^T F\, G^{-1} \left\{ F^T \begin{bmatrix} z \\ V_z \end{bmatrix} + \int_t^{t_f} F^T \begin{bmatrix} 0 \\ -cV_{tz} + a_{tz} \end{bmatrix} \mathrm{d}s \right\} \tag{5}$$

where

$$\dot{F} = -A^T F, \qquad F(t_f) = \begin{bmatrix} 1 \\ 0 \end{bmatrix} \tag{6}$$

$$G(t) = -\int_t^{t_f} w^{-1}(s) F^T(s) B\, B^T F(s)\, \mathrm{d}s \tag{7}$$

$$A = \begin{bmatrix} 0 & 1 \\ 0 & c \end{bmatrix}, \qquad B = \begin{bmatrix} 0 \\ -1 \end{bmatrix}$$

These equations are solved to give

$$F(t) = \begin{bmatrix} 1 \\ t_g(t) \end{bmatrix}, \qquad G(t) = -\int_t^{t_f} w^{-1}(s) t_g^2(s)\, \mathrm{d}s \tag{8}$$

where

$$t_g(t) = \frac{\int_t^{t_f} V_m(s)\, \mathrm{d}s}{V_m(t)} \tag{9}$$

and therefore

$$u_z(t) = -\frac{w^{-1}(t) t_g(t)}{G(t)} \left[z(t) + t_g(t) V_z(t) - \int_t^{t_f} c(s) t_g(s) V_{tz}(s)\, \mathrm{d}s + \int_t^{t_f} t_g(s) a_{tz}(s)\, \mathrm{d}s \right] \tag{10}$$

Equation (10) can be put into the form

$$u_z(t) = \frac{N(t)}{t_g^2(t)} \cdot \mathrm{ZEM} \tag{11}$$

where ZEM denotes the zero-effort miss [the term in brackets in Eq. (10)] and the guidance gain $N(t)$ is defined as

$$N(t) = -\frac{w^{-1}(t) t_g^3(t)}{G(t)} = \frac{w^{-1}(t) t_g^3(t)}{\int_t^{t_f} w^{-1}(s) t_g^2(s)\, \mathrm{d}s} \tag{12}$$

The optimal control u_z can be expressed in an alternative form by using the costate of the above optimal control problem.[4] Indeed, the same argument as in Ref. 2 leads to the following representation of u_z:

$$u_z(t) = \nu w^{-1}(t) B^T F(t) = \nu w^{-1}(t) t_g(t) \tag{13}$$

where ν is a constant parameter. Because t_g goes to 0 as t approaches t_f, it is clear that these guidance commands decrease to 0 in the final stage of engagement. This is a desirable property because there will be enough room for acceleration command in the final moments to cope with the various uncertainties and disturbances encountered in actual engagement. Note that the PNG law cannot keep this property when missile velocity varies.

If the flight envelope is either subsonic or supersonic, we only need to consider the case $w(t) = \rho^{-\alpha}(t) v_m^{-\beta}(t)$. Let us denote the guidance gain for this case by $N_{\alpha\beta}$; thus,

$$N_{\alpha\beta}(t) = \frac{t_g^3(t)}{\int_t^{t_f} r_{\alpha\beta}(s;t) t_g^2(s)\, \mathrm{d}s} \tag{14}$$

where

$$r_{\alpha\beta}(s;t) = \left[\frac{\rho(s)}{\rho(t)} \right]^{\alpha} \left[\frac{V_m(s)}{V_m(t)} \right]^{\beta}, \qquad \text{for} \quad s \geq t$$

Note that the optimal guidance laws parameterized by α and β differ from each other only in their guidance gains $N_{\alpha\beta}$. Therefore, qualitative characteristics of the way that $N_{\alpha\beta}$ behaves according to the value of α and β are investigated in the next section.

Before leaving this section, we briefly discuss the limiting case of $\alpha \to \infty$ or $\beta \to \infty$. First, note that, from the Eqs. (11), (13), and (14),

$$\nu = \frac{\mathrm{ZEM}(0)}{\int_0^{t_f} \rho^{\alpha}(s) V_m^{\beta}(s) t_g^2(s)\, \mathrm{d}s} \tag{15}$$

and therefore

$$u_z(t) = \frac{t_g(t) \mathrm{ZEM}(0)}{\int_0^{t_f} r_{\alpha\beta}(s;t) t_g^2(s)\, \mathrm{d}s} \tag{16}$$

It is then easy to see that in the limiting case of $\beta \to \infty$, $u_z(t) = \infty$ if $V_m(t) = \max_{0 \leq s \leq t_f} V_m(s)$, and $u_z(t) = 0$ otherwise. A similar conclusion holds for the limiting case of $\alpha = \infty$.

III. Properties of Guidance Gains $N_{\alpha\beta}(t)$

In this section, we investigate the characteristics of $N_{\alpha\beta}(t)$ for the case of $w(t) = \rho^{-\alpha}(t) v_m^{-\beta}(t)$ with α and β being constant. Define

$$\eta(t) \equiv \frac{t_g(t)}{t_{\mathrm{go}}(t)}, \qquad \eta_{\min}(t) \equiv \min_{t \leq s \leq t_f} \eta(s)$$

$$\eta_{\max}(t) \equiv \max_{t \leq s \leq t_f} \eta(s), \qquad r_{\min}(t) \equiv \min_{t \leq s \leq t_f} r_{\alpha\beta}(s;t)$$

$$r_{\max}(t) \equiv \max_{t \leq s \leq t_f} r_{\alpha\beta}(s;t)$$

We first state the following property shown in Ref. 2.

Property 1 (Ref. 2):

i) $\eta(t) > 0$.

ii) $\lim_{t \to t_f} \eta(t) = 1$.

Now we are ready to prove Property 2.

Property 2: For any α, β,

i) $3\eta^3(t)/[r_{\max}(t)\, \eta_{\max}^2(t)] \leq N_{\alpha\beta}(t) \leq 3\eta^3(t)/[r_{\min}(t) \eta_{\min}^2(t)]$

ii) $\lim_{t \to t_f} N_{\alpha\beta}(t) = 3$

Proof:

i) Note that for $t \leq s \leq t_f$,

$$t_{\mathrm{go}}^2(s) \eta_{\min}^2(t) \leq t_g^2(s) = t_{\mathrm{go}}^2(s) \eta^2(s) \leq t_{\mathrm{go}}^2(s) \eta_{\max}^2(t)$$

Also,

$$r_{\min}(t) \int_t^{t_f} t_g^2(s)\, \mathrm{d}s \leq \int_t^{t_f} r_{\alpha\beta}(s;t) t_g^2(s)\, \mathrm{d}s \leq r_{\max}(t) \int_t^{t_f} t_g^2(s)\, \mathrm{d}s$$

Hence

$$r_{\min}(t) \eta_{\min}^2(t) \int_t^{t_f} t_{\mathrm{go}}^2(s)\, \mathrm{d}s \leq \int_t^{t_f} r_{\alpha\beta}(s;t) t_g^2(s)\, \mathrm{d}s \leq r_{\max}(t) \eta_{\max}^2(t) \int_t^{t_f} t_{\mathrm{go}}^2(s)\, \mathrm{d}s$$

Because

$$\int_t^{t_f} t_{\mathrm{go}}^2(s)\, \mathrm{d}s = \left(\frac{1}{3} \right) t_{\mathrm{go}}^3(t)$$

and $t_g^3(t) = t_{\mathrm{go}}^3(t) \eta^3(t)$, the conclusion follows.

ii) Because $\lim_{t \to t_f} r_{\max}(t) = \lim_{t \to t_f} r_{\min}(t) = 1$, the conclusion follows from i) and Property 1. |

Now we investigate how $N_{\alpha\beta}$ varies according to the values of α and β. First, we fix α and define

$$D_{\beta}(t) \equiv \int_t^{t_f} r_{\alpha\beta}(s;t) t_g^2(s)\, \mathrm{d}s$$

Then $N_{\alpha\beta} = t_g^3 / D_{\beta}$. Let

$$D_{\beta_1\beta_2}(t) \equiv D_{\beta_1}(t) - D_{\beta_2}(t), \qquad \beta_1, \beta_2 > 0, \quad \beta_1 \neq \beta_2$$

Write $D_{\beta_1\beta_2}$ as

$$D_{\beta_1\beta_2}(t) = \frac{1}{\rho^{\alpha}(t) V_m^{\beta_1}(t)} E_{\beta_1\beta_2}(t)$$

where

$$E_{\beta_1\beta_2}(t) \equiv \int_t^{t_f} \rho^{\alpha}(s)\left\{V_m^{\beta_1-\beta_2}(s) - V_m^{\beta_1-\beta_2}(t)\right\}V_m^{\beta_2}(s)t_g^2(s)\,\mathrm{d}s \tag{17}$$

It is then clear that $N_{\alpha\beta_1} < N_{\alpha\beta_2}$ if and only if $E_{\beta_1\beta_2} > 0$.

Property 3: For $\beta_1 > \beta_2$,

i) If $\dot{V}_m(s) \geq 0$ for all $s \in [t, t_f]$, then $N_{\alpha\beta_1}(s) \leq N_{\alpha\beta_2}(s)$ for all $s \in [t, t_f]$.

ii) If $\dot{V}_m(s) \leq 0$ for all $s \in [t, t_f]$, then $N_{\alpha\beta_1}(s) \geq N_{\alpha\beta_2}(s)$ for all $s \in [t, t_f]$.

Proof:

i) The hypothesis implies that $V_m(s) \geq V_m(t)$ for all $s \in [t, t_f]$. By the definition of $E_{\beta_1\beta_2}$, we have $E_{\beta_1\beta_2}(s) \geq 0$ for all $s \in [t, t_f]$. Hence the conclusion follows.

ii) The same argument as in i) leads to the conclusion. ∎

A similar argument leads to Property 4.

Property 4: For $\alpha_1 > \alpha_2$,

i) If $\dot{\rho}(s) \geq 0$ for all $s \in [t, t_f]$, then $N_{\alpha_1\beta}(s) \leq N_{\alpha_2\beta}(s)$ for all $s \in [t, t_f]$.

ii) If $\dot{\rho}(s) \leq 0$ for all $s \in [t, t_f]$, then $N_{\alpha_1\beta}(s) \geq N_{\alpha_2\beta}(s)$ for all $s \in [t, t_f]$.

In many applications, the missile altitude or the air density varies monotonically. Therefore, Property 4 could be used as a useful guideline for choosing the value of α. Indeed, if ρ is decreasing, the optimal guidance gain is larger with a larger α, so that the missile tries harder to reduce ZEM before the air density becomes too low, which coincides with the physical intuition. The missile velocity, however, usually is not monotonic because many missiles have both boosting and coasting phases. Thus we need a more useful property than Property 3 to describe the behavior of $N_{\alpha\beta}$ for different values of β. For this, let α again be fixed.

Property 5: Suppose that for some $t_b \in [0, \infty)$, $\dot{V}_m(t) > 0$ for $t \leq t_b$ and $\dot{V}_m(t) < 0$ for $t > t_b$. Then, for $\beta_1 > \beta_2$,

i) If $t_f \leq t_b$, then $N_{\alpha\beta_1}(t) < N_{\alpha\beta_2}(t)$ for all $t < t_f$.

ii) If $t_b < t_f$, then either (a) or (b) holds:

a) There exists $t_{\beta_1\beta_2} < t_b$ such that $E_{\beta_1\beta_2}(t_{\beta_1\beta_2}) = 0$, and

$$N_{\alpha\beta_1}(t) < N_{\alpha\beta_2}(t) \quad \text{for} \quad t < t_{\beta_1\beta_2}$$

$$N_{\alpha\beta_1}(t) = N_{\alpha\beta_2}(t) \quad \text{for} \quad t = t_{\beta_1\beta_2}$$

$$N_{\alpha\beta_1}(t) > N_{\alpha\beta_2}(t) \quad \text{for} \quad t_{\beta_1\beta_2} < t < t_f$$

b) $N_{\alpha\beta_1}(t) > N_{\alpha\beta_2}(t)$ for all $t < t_f$.

Proof:

i) Consider $E_{\beta_1\beta_2}$ defined by Eq. (17). Note that

$$\dot{E}_{\beta_1\beta_2}(t) = -(\beta_1 - \beta_2)V_m^{\beta_1-\beta_2-1}(t)\dot{V}_m(t)\int_t^{t_f} \rho^{\alpha}(s)V_m^{\beta_2}(s)t_g^2(s)\,\mathrm{d}s$$

Therefore, for all $t < t_f$,

$$\dot{E}_{\beta_1\beta_2}(t) < 0 \quad \text{if} \quad \dot{V}_m(t) > 0$$

$$\dot{E}_{\beta_1\beta_2}(t) > 0 \quad \text{if} \quad \dot{V}_m(t) < 0$$

Because $t_f \leq t_b$, $\dot{V}_m(t) > 0$ for all $t < t_f$ by the hypothesis so that $E_{\beta_1\beta_2}(t)$ is strictly decreasing in the interval $[0, t_f)$. Now that $E_{\beta_1\beta_2}(t_f) = 0$, $E_{\beta_1\beta_2}(t) > 0$ for all $t < t_f$, and therefore $N_{\alpha\beta_1}(t) < N_{\alpha\beta_2}(t)$ for all $t < t_f$.

ii) Because V_m is strictly decreasing in (t_b, t_f), we have from the definition of $E_{\beta_1\beta_2}$ that $E_{\beta_1\beta_2}(t_b) < 0$. By the same reasoning as in the preceding i), we deduce that $E_{\beta_1\beta_2}(t)$ strictly decreases to the minimum value $E_{\beta_1\beta_2}(t_b) < 0$ as t increases to t_b, and then strictly increases to 0 as t approaches t_f. If $E_{\beta_1\beta_2}(0) \geq 0$, then there exists, by the continuity of $E_{\beta_1\beta_2}(t)$, $t_{\beta_1\beta_2} < t_b$ such that $E_{\beta_1\beta_2}(t_{\beta_1\beta_2}) = 0$; in this case, $E_{\beta_1\beta_2}(0) > 0$ for $t < t_{\beta_1\beta_2}$ and $E_{\beta_1\beta_2}(0) < 0$ for $t > t_{\beta_1\beta_2}$, which implies conclusion a. If $E_{\beta_1\beta_2}(0) < 0$, then we must have that $E_{\beta_1\beta_2}(t) < 0$ for all $t < t_f$, and therefore that $N_{\alpha\beta_1}(t) > N_{\alpha\beta_2}(t)$ for all $t < t_f$, which is conclusion b. ∎

Note that the hypothesis in Property 5 describes a typical acceleration profile of surface-to-air missiles that have an initial boosting phase with the burnout time t_b followed by a coasting phase. Note also that $t_{\beta_1\beta_2}$ exists whenever the missile terminal velocity is larger than the initial velocity (the missile velocity at the time of guidance initiation), which is true in most surface-to-air missile applications: Indeed, as argued in the proof of Property 5, $E_{\beta_1\beta_2}(0) > 0$ is an equivalent statement to the existence of such $t_{\beta_1\beta_2}$, and it is clear from the definition that $E_{\beta_1\beta_2}(0) > 0$ if $V_m(s) > V_m(0)$ for all $s > 0$.

Now let us restrict ourselves to the case in which the air density is constant, e.g., as in a horizontal engagement scenario, and β takes the value from 0, 1, and 2. For brevity, we use the notation N_β for $N_{\alpha\beta}$. In view of Property 5, we then see that, in most surface-to-air missile applications,

$$N_0(t) > N_1(t) > N_2(t) \quad \text{in the first part of the boosting phase}$$

$$N_0(t) < N_1(t) < N_2(t) \quad \text{from the latter part of the boosting phase}$$

In particular, note that the drag-minimizing guidance laws ($\beta = 1$ or 2) use smaller guidance gains than the control-effort minimizing law ($\beta = 0$) in the beginning of the engagement. Because the magnitude of acceleration that a missile can exert often is limited severely in the beginning of the boosting phase because of low missile velocity, the drag-minimizing guidance laws can be used not only for drag minimization but also as a practical guidance scheme that accounts for the limited lift capability in the initial guidance stage.

IV. Implementation Issues

To implement the optimal guidance laws developed in this paper, the missile needs the following information: a) current relative position and relative velocity between the missile and the target, b) current target velocity vector and future target acceleration profile, and c) future missile velocity and air density profiles. Because future target acceleration is unknown, we usually assume for a practical reason that the current target acceleration is maintained throughout the engagement. Once all of the preceding information is obtained, we can compute the key variables in the guidance command (11) such as t_g, $N_{\alpha\beta}$, t_{go}, and ZEM. In particular, t_{go} can be computed as a numerical solution that satisfies

$$\left[\int_t^{t+t_{\mathrm{go}}} V_m(s)\,\mathrm{d}s\right]^2 = \frac{1}{4}a_t^2(t)t_{\mathrm{go}}^4 + V_t(t)a_t(t)t_{\mathrm{go}}^3 + \left\{a_t(t)R(t)\cos[\sigma_t(t) - \sigma(t)] + V_t^2(t)\right\}t_{\mathrm{go}}^2 + 2R(t)V_t(t)\cos[\sigma_t(t) - \sigma(t)]t_{\mathrm{go}} + R^2(t) \tag{18}$$

(This t_{go} computation method is based on the assumption that the missile instantly nullifies its heading error to return to the collision path at every instant; for the derivation of the equation, see Ref. 1 or 2.)

Note that items a and b at the beginning of this section are the information required for many modern optimal homing guidance laws. Item a can be determined by using the active seeker outputs (see Ref. 2), and b can be estimated in a target tracking filter. Estimation errors of the target tracking filter may cause a significant degradation of the guidance performance. However, this issue, which is common to any modern guidance law, is not investigated further because it is beyond the scope of this paper.

Item c is the additionally required information by which the proposed optimal guidance laws differ from most other guidance laws. Because it is not possible to obtain the exact information of c, we have to use some predicted profiles in actual guidance-law implementation. Discrepancy between true and predicted profiles of c could severely degrade the guidance performance. In particular, the error in the predicted missile velocity profile results in wrong guidance gains and, more frequently, erroneous time-to-go estimates; the latter is a most critical factor that makes the guidance command blow up in the last moment of engagement. On the other hand, the effect of an error in the predicted air density profile is confined to the computation of guidance gain. As a result, an inaccurate air density profile results in some deviation from the optimal guidance gain, but the resulting guidance algorithm maintains the nice property that the guidance command decreases to zero in the final stage of engagement. Thus we assume from now on that we perfectly know

items a and b, and we concentrate on the investigation of the effect of uncertainty in the future velocity profile. We suggest a couple of velocity-profile update schemes that can be used effectively when the current missile velocity is available.

Let us denote a missile velocity profile predicted before launch as $\{\bar{V}_m(s),\ 0 \le s \le t_f\}$. Note that even if we use $\{\bar{V}_m\}$ instead of $\{V_m\}$ in computing $N_{\alpha\beta}$, Properties 2 through 5 still hold with V_m in the Properties interpreted as $\bar{V}_m$. In particular, if $\bar{V}_m(t) = \bar{k}\, V_m(t)$, $\bar{k}$ is constant, then we get exactly the same values of t_g and $N_{\alpha\beta}$ as in the case of using the true missile velocity profile. However, as shown in the next section, the guidance command could blow up in the final stage of engagement when $\{\bar{V}_m\}$ is different from the true one, which is mainly due to the erroneous t_{go} computation resulting from the use of a wrong velocity profile.

Now assume that the current missile velocity is known. In this case, we could use one of the simple velocity profile update schemes elaborated in the following, considerably alleviating the problem of guidance command blowup caused by incorrect missile velocity profiles.

i) When $\bar{V}_m$ is given by some function of time and the present velocity; i.e., $\bar{V}_m(s) = f(s,\ \bar{V}_m(t))$ for $s \ge t$: Note that the case in which $\bar{V}_m$ is given by some differential equations belongs to this category. In this case, we can update the future velocity profile simply by setting $\bar{V}_m(s) = f(s, V_m(t))$, $s \ge t$, at each time instant t; i.e., by replacing the initial value $\bar{V}_m(t)$ of the function f with the current missile velocity, as proposed in Ref. 5.

ii) For any form of $\{\bar{V}_m\}$ including tabular forms: At each time t, we define

$$k(t) \equiv \frac{V_m(t)}{\bar{V}_m(t)}$$

and redefine the predicted velocity profile according to the scale of $k(t)$; i.e., let

$$\bar{V}_m^{\text{new}}(s) = k(t)\, \bar{V}_m^{\text{old}}(s), \qquad \text{for} \quad s \ge t$$

As discussed earlier, scaling of the velocity profile does not change the values of t_g and $N_{\alpha\beta}$; however, it changes the value of the t_{go} estimate.

The preceding velocity-profile update schemes are simple and straightforward, but turn out to be quite effective as shown in the computer simulation study.

V. Numerical Examples

In this section, we conduct two simulation studies for antiaircraft missile engagements to demonstrate the effectiveness of the proposed guidance method. First, the proposed guidance laws are compared with the existing ones in the guidance performance of a supersonic missile under the presence of velocity profile inaccuracies and guidance system lags. The usefulness of the proposed update schemes also are examined. Next, a drag minimization problem for a surface-to-air missile that is accelerated from a subsonic speed to a supersonic one is investigated. For all of the numerical examples, a horizontal engagement is assumed for simplicity, and therefore, the air density in the cost function plays no role in these studies.

A. Effects of Velocity Uncertainties and Guidance Lags

In this simulation study, we are concerned with the divergence problem due to velocity-profile prediction errors as well as with the effectiveness of the proposed update schemes. The effect of induced drag on the missile speed is ignored, for simplicity. The missile velocity profile is chosen as $V_m(0) = 340$ m/s, $\dot{V}_m(t) = 340$ m/s^2 for $0 \le t \le 2$ s, and $\dot{V}_m(t) = -\frac{1}{10} V_m(t)$ for $t > 2$ s. The initial conditions of the engagement are given by $\sigma_m(0) = 45$ deg, $x(0) = 8$ km, $z(0) = 0$, and $\sigma_t(0) = 135$ deg. The target is turning with a constant speed; $V_t(t) = 340$m/s and $a_t(t) = -2.5g$ for all t. The prefect collision-path angle is computed as $\sigma_L = 29.7$ deg; hence, the missile has an initial heading error of 15.3 deg. Given the missile velocity profile, we can compute the guidance gains N_β, which are displayed in Fig. 2 for $t_f = 11.23$ s: In this figure, we see that the N_β behave as stated in Properties 2, 3, and 5. We have applied to this scenario the augmented proportional navigation guidance (APNG) law with $N = 3$:

$$u_z(t) = \frac{N}{t_{\text{go}}^2(t)} \left\{ z(t) + t_{\text{go}}(t) V_z(t) + \frac{1}{2} t_{\text{go}}^2(t) a_{tz}(t) \right\}$$

and Baba's algorithm (specifically, APXGL with $N = 5$ in Ref. 1) as well as the optimal guidance law presented in this paper. Only the cases $\beta = 0$, $\beta = 1$, and $\beta = 2$ have been considered for the optimal guidance law. As for the t_{go} computation, we have used an approximation $t_{\text{go}} \approx x / V_{cx}$, where V_{cx} is the x-axis component of the closing velocity, for APNG, and Eq. (18) for the rest of the guidance laws.

Six cases are considered to assess the performance of the proposed guidance algorithms. In all cases, the relative geometry (z and V_z) and the target states (V_t, a_t, and σ_t) are assumed to be known:

Case 1: No guidance system lag, perfect knowledge of the missile future velocity profile.

Case 2: No guidance system lag, missile velocity is not available, and the predicted profile is given by

$$\dot{\bar{V}}_m = 300\,\text{m/s}^2 \qquad \text{for} \qquad 0 \le t \le \bar{t}_b$$

$$\dot{\bar{V}}_m = -\tfrac{1}{12} \bar{V}_m \qquad \text{for} \qquad t > \bar{t}_b$$

where $\bar{t}_b = 2.267$ s.

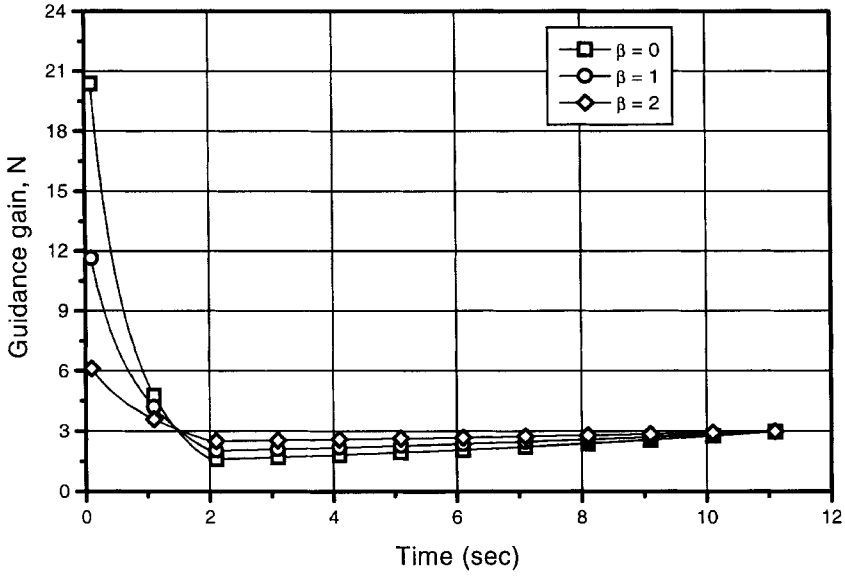

Fig. 2 Guidance gains N_β.

Case 3: No guidance system lag, current missile velocity is available, and the predicted profile of case 2 with update scheme (i) from the preceding section is used.

Case 4: Same as case 3, but velocity update scheme (ii) is used.

Case 5: Perfect knowledge of the future missile velocity profile, guidance system lag modeled by $1/(s+1)$.

Case 6: Same as case 3 except that the guidance system lag is modeled by $1/(s+1)$.

First, consider case 1. As shown in Fig. 3, the guidance commands decrease to zero in all optimal guidance laws as t approaches the final impact instant, which is expected from Eq. (13). On the other hand, the guidance command in APNG does not go to zero. We also have computed the values of various costs for case 1 and summarize the results in Table 1, which clearly validate the derivation of the optimal guidance laws.

When we use an inaccurately predicted missile velocity profile (case 2), the guidance commands of the optimal guidance laws rapidly diverge as the missile approaches the target, as shown in Fig. 4. This undesirable phenomenon is improved considerably if we employ either of the two velocity-profile updating schemes using the current missile velocities (see Figs. 5 and 6). Note that the command histories of the optimal guidance laws in Figs. 5 and 6 are not much different in their shape from those in Fig. 3; small nonzero values of guidance commands at the impact instant are the only noticeable effect of an inaccurate missile velocity profile when a velocity update scheme is used.

If there is a guidance system lag (cases 5 and 6), the optimal guidance commands abruptly diverge at the very last moments, but maintain in most time the same shape and properties as in the case of no guidance system lag, as observed in Figs. 7 and 8. In particular, the incorrect missile velocity profile, if used with the velocity update scheme (i), does not exacerbate the effect of a guidance system lag. A miss-distance analysis has been performed for cases 5 and 6 by repeatedly running computer simulations for various total engagement times t_f, i.e., for various initial ranges $x(0)$, and its results are displayed in Figs. 9 and 10. The miss distances of the optimal guidance laws for case 6 are comparable to those for case 5, and far better than that of APNG.

Table 1 Cost values of various guidance laws (case 1)

Cost function	Optimal guidance laws $\beta=0$	$\beta=1$	$\beta=2$	Baba, $N=5$	APNG, $N=3$
$\int_0^{t_f} u^2\,dt$	**12,627**	13,158	15,551	19,990	96,137
$\int_0^{t_f} u^2/V_m\,dt$	22.66	**19.60**	20.11	23.86	148.95
$\int_0^{t_f} u^2/V_m^2\,dt$	0.045	0.032	**0.028**	0.030	0.266

B. Drag Minimization

Consider a realistic missile flight with a boost phase and a coast phase. The initial speed is $V_m(0)=100$ m/s, and the longitudinal acceleration is given by $\dot{V}_m = A_T - \mu V_m^2 C_D$ during the boost phase ($0 \le t \le 2.5$ s) and $\dot{V}_m = -\mu V_m^2 C_D$ after the booster burnout ($t > 2.5$ s). The acceleration due to thrust is given by $A_T = 380$ m/s^2

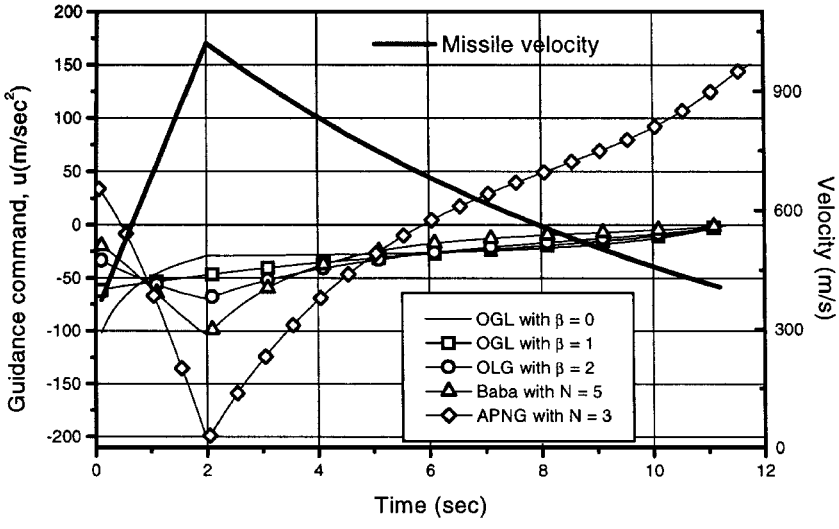

Fig. 3 Guidance commands with true velocity profile (case 1).

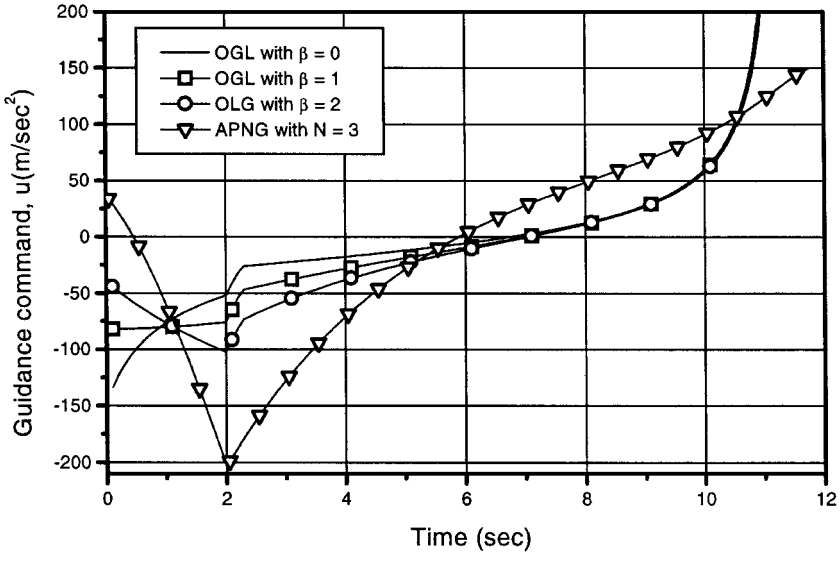

Fig. 4 Guidance commands with predicted velocity profile (case 2).

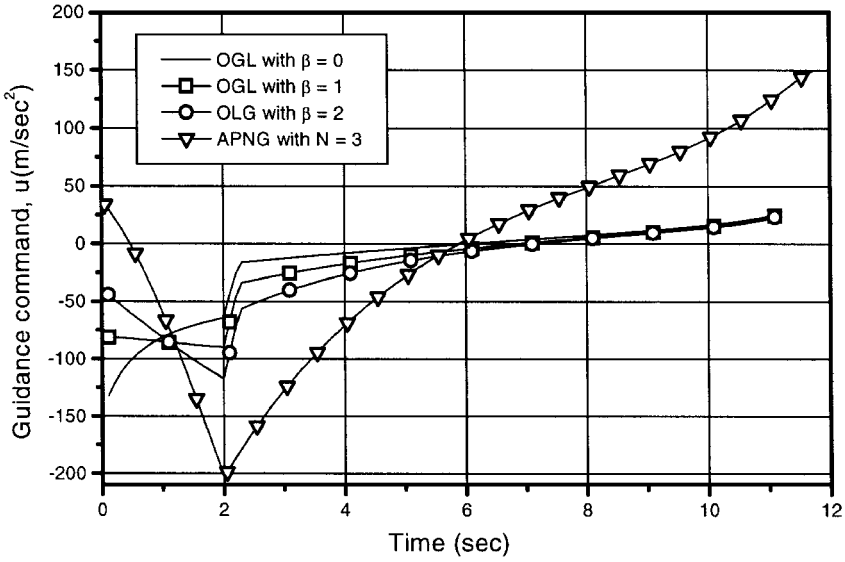

Fig. 5 Guidance commands with velocity profile update scheme (i) (case 3).

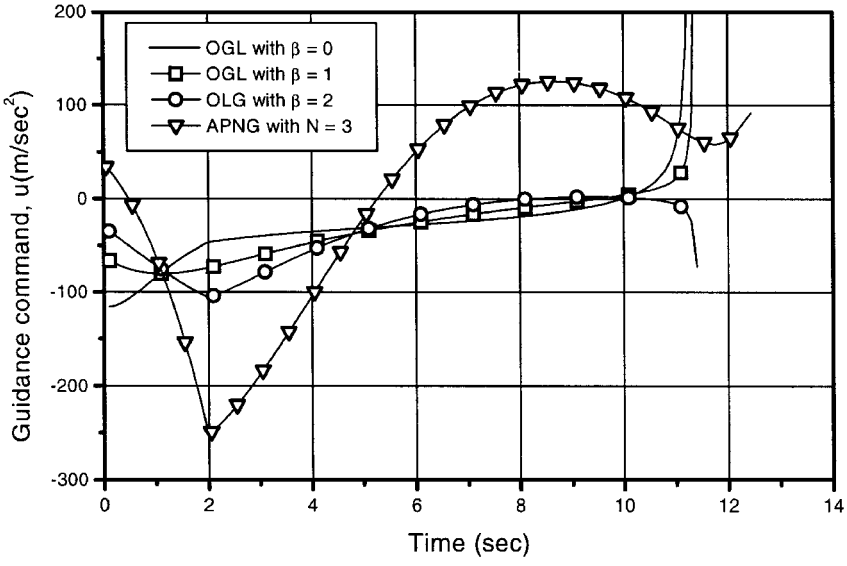

Fig. 6 Guidance commands with velocity profile update scheme (ii) (case 4).

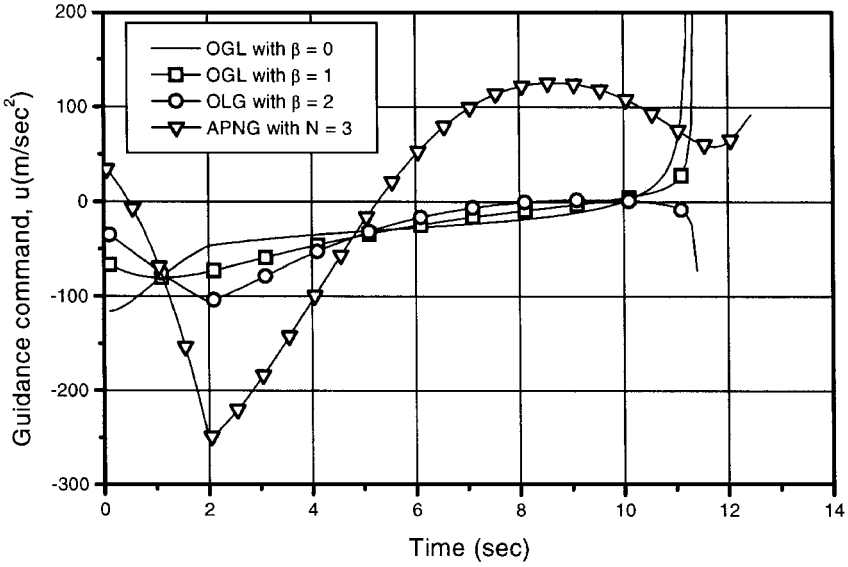

Fig. 7 Guidance commands with guidance lag and true velocity profile (case 5).

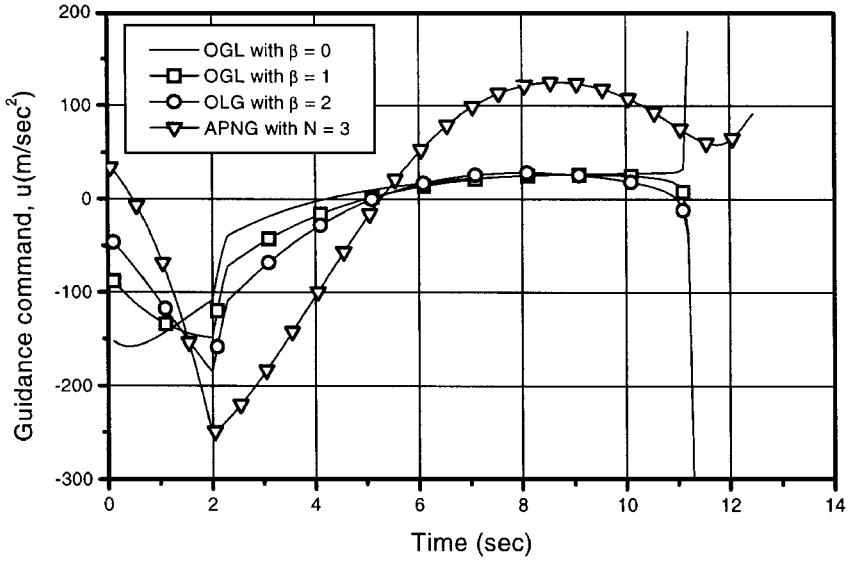

Fig. 8 Guidance commands with guidance lag and predicted velocity profile update (case 6).

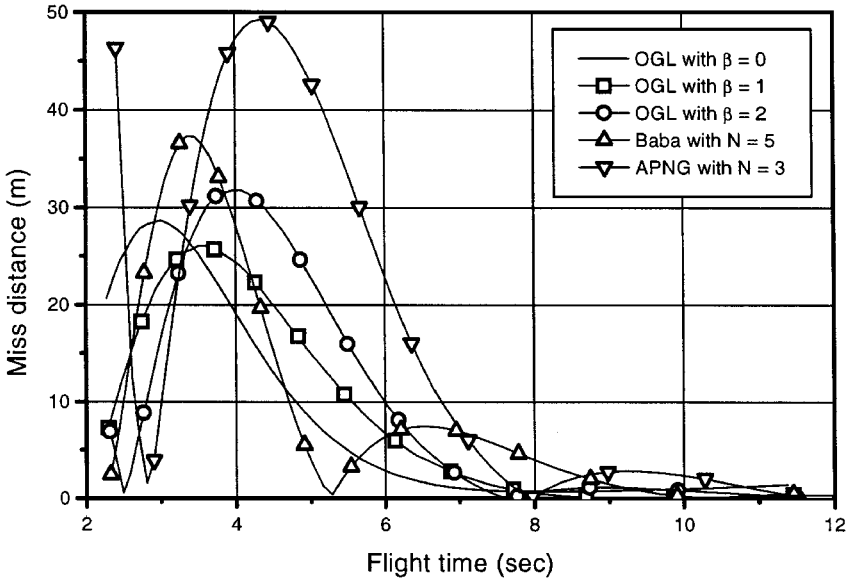

Fig. 9 Miss distances (case 5).

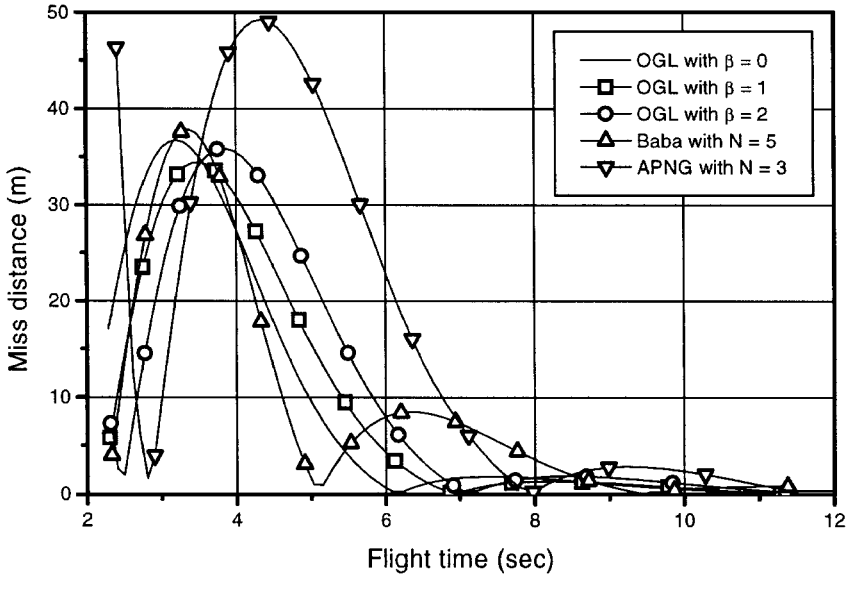

Fig. 10 Miss distances (case 6).

and the coefficient μ is chosen as $1/6000\ \mathrm{m}^{-1}$. Because of the booster thrust, the missile exceeds the sonic speed within 0.7 s and obtains the burnout velocity of almost 1000 m/s. The drag characteristics are given by

$$C_{D_o}(M) = \begin{cases} 0.45 & \text{for} \quad M \le 0.95 \\ \dfrac{0.5}{\sqrt{M^2-1}} & \text{for} \quad M \ge 1.05 \end{cases}$$

$$k_i(M) = \begin{cases} 0.1 & \text{for} \quad M \le 0.95 \\ \dfrac{\sqrt{M^2-1}}{4} & \text{for} \quad M \ge 1.05 \end{cases}$$

The values of C_{D_o} and k_i for the transonic region are calculated by the interpolation of the data at $M = 0.95$ and 1.05. The missile velocity profile required for guidance computation is calculated in advance by assuming $C_L = 0$, and the update scheme (ii) is employed during the engagement.

The target initially is located at $x(0) = 12$ km and $z(0) = 0$ km, and travels along a straight course at a speed of 340 m/s with $\sigma_t = 135$ deg. For this scenario, four guidance laws are compared: three guidance laws with the guidance gains for $\beta = 0$, 1, 2, respectively, and the drag-minimizing guidance law, which is a dual-gain guidance law taking the drag characteristics in the two speed regions into account. Because a horizontal engagement is assumed, the air density and the speed of sound are constant. Hence, the weighting function is chosen as $w(t) = k_i(M)/M^2$.

Table 2 shows the missile's terminal velocity for several values of the initial missile heading. As expected, the dual-gain guidance law gives the highest terminal velocity for all cases. Note that the effectiveness of the dual-gain guidance law is significant when the initial heading error is large: $\sigma_m(0) = 45$ deg. For this case, the missile needs to maneuver more than for the other cases, producing

Table 2 Terminal velocity for various guidance laws (m/s)

Guidance law	$\sigma_m(0) =$ 0 deg	$\sigma_m(0) =$ 15 deg	$\sigma_m(0) =$ 30 deg	$\sigma_m(0) =$ 45 deg
$\beta = 0$	642.0	749.3	725.4	652.3
$\beta = 1$	708.2	751.0	731.5	665.8
$\beta = 2$	679.9	750.8	721.9	638.5
Dual gain	712.9	751.2	733.4	674.3

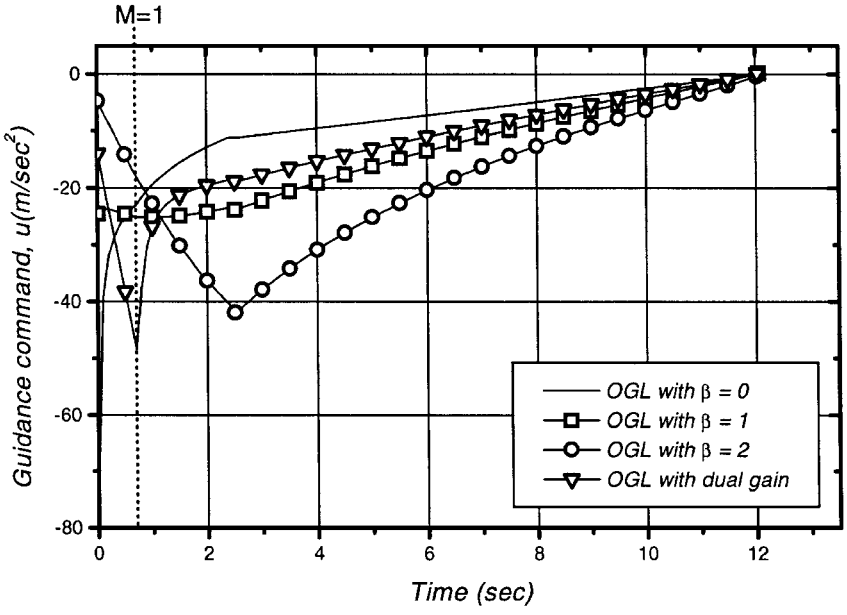

Fig. 11 Guidance commands for $\sigma_m(0) = 30$ deg.

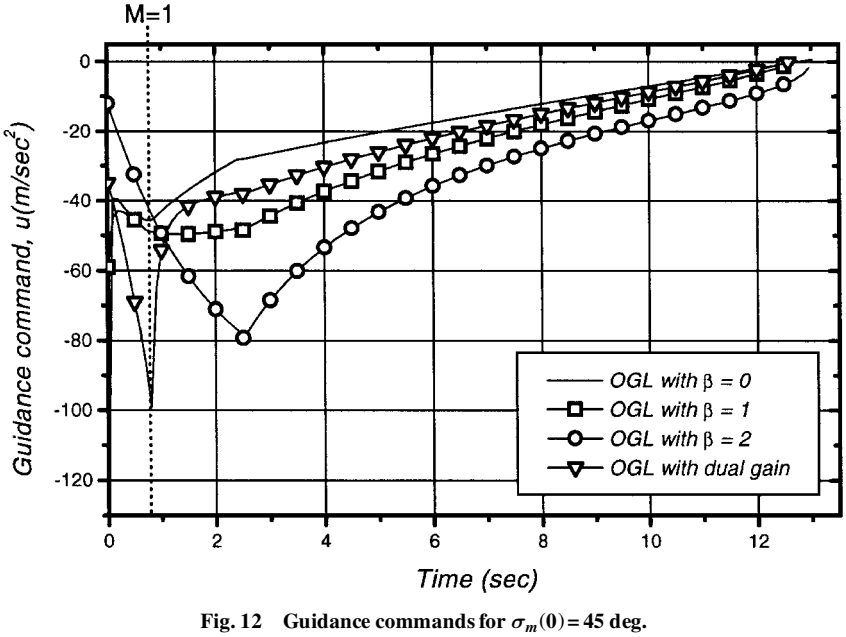

Fig. 12 Guidance commands for $\sigma_m(0) = 45$ deg.

Table 3 Burnout velocity for various guidance laws (m/s)

Guidance law	$\sigma_m(0) =$ 0 deg	$\sigma_m(0) =$ 15 deg	$\sigma_m(0) =$ 30 deg	$\sigma_m(0) =$ 45 deg
$\beta = 0$	899.6	1001.7	979.1	921.2
$\beta = 1$	978.6	1003.0	991.3	951.8
$\beta = 2$	984.5	1003.2	993.4	960.4
Dual gain	976.8	1003.0	990.6	950.4

more maneuver-induced drag. It also is observed that the wave-drag minimization guidance law ($\beta = 1$) gives the second-best result for all cases because most of the flight region is supersonic. Figures 11 and 12 show the time history of each guidance command for $\sigma_m(0) = 30$ deg and 45 deg, respectively. It is observed in these figures that the guidance commands produced by the conventional control-effort minimizing law ($\beta = 0$) are far from the optimal ones for drag minimization. At high subsonic speeds, the dual-gain guidance law produces the largest missile maneuver among the four guidance laws. Because the induced drag in the subsonic region is assumed to be inversely proportional to the dynamic pressure, it is more advantageous for drag reduction to maneuver in the high subsonic region rather than the low subsonic region. On the other hand, the control-effort minimizing guidance law ($\beta = 0$) does not consider this fact so as to produce large guidance commands in the beginning, resulting in the largest velocity loss at burnout, as shown in Table 3. That explains why this guidance law does not give the highest terminal velocity even though its guidance commands remain the smallest for the rest of the flight.

VI. Concluding Remarks

A class of weighted control-effort minimizing guidance laws are derived for varying-velocity missiles. In particular, we extensively study the case in which the weighting function is given in the form of $\rho^{-\alpha} V_m^{-\beta}$. The resulting guidance law could represent a drag-minimizing law for subsonic missiles (for $\alpha = 1$, $\beta = 2$) or supersonic missiles (for $\alpha = 1, \beta = 1$). Furthermore, the same formulation enables us to solve the drag minimization problem for a missile system of arbitrary velocity range and drag characteristics. Therefore, it gives a guidance-law designer much flexibility to account for specific needs and/or constraints of missiles in a simple manner.

The optimal guidance law of this paper, as well as any optimal guidance law that explicitly accounts for missile speed variation in its problem formulation, needs to use some form of future missile velocity profile that obviously is not exactly known during the engagement. We have shown that although an inaccurate velocity profile makes guidance commands diverge at the final stage of engagement, simple on-line velocity-profile update schemes can effectively alleviate the problem. Also, a miss-distance analysis is performed for the case of guidance system lag, and reveals that the optimal guidance laws perform far better than the conventional APNG law. Finally, a drag minimization problem for a typical surface-to-air missile system is solved to demonstrate the usefulness of the proposed method for practical missile guidance. The iterative computation for t_{go} estimation could be a burden for some applications. A study on computationally efficient t_{go} estimation methods is under way.

Acknowledgments

The authors are very grateful to three anonymous reviewers for their valuable comments that have been very helpful in revising this paper.

References

[1] Baba, Y., Takehira, T., and Takano, H., "New Guidance Law for a Missile with Time Varying Velocity," *Proceedings of the AIAA Guidance, Navigation, and Control Conference*, AIAA, Washington, DC, 1994, pp. 207–215.

[2] Cho, H., Ryoo, C. K., and Tahk, M. J., "Closed-Form Optimal Guidance Law for Missiles of Time-Varying Velocity," *Journal of Guidance, Control, and Dynamics*, Vol. 19, No. 5, 1996, pp. 1017–1022.

[3] "Properties of a Standard Atmosphere," Item No. 77021, Engineering Science Data Unit, Royal Aeronautical Society, London, 1977.

[4] Bryson, A. E., and Ho, Y. C., *Applied Optimal Control,* Wiley, New York, 1975, Chap. 5.

[5] Ryoo, C. K., Cho, H., and Tahk, M. J., "Performance Characteristics of Linear Optimal Guidance Laws for Varying Velocity Missiles," *Proceedings of 2nd Asian Control Conference* (Seoul, Korea), Vol. 2, 1997, pp. 395–398.